

On the Mechanism of Oxalic Acid Oxidation on Iron-doped TiO₂ Photocatalysts

A.I. Kokorin¹, R. Amal², W.Y. Teoh², A.I. Kulak³

¹*N.Semenov Institute of Chemical Physics RAS, Kosygin Str. 4, 119991 Moscow, Russia*

²*School of Chemical Sciences and Engineering, UNSW, Sydney, NSW 2052, Australia*

³*Institute of General and Inorganic Chemistry NASB, Surganova Str. 9, 220072 Minsk, Belarus*

One of the principal problems for practical application of TiO₂ materials in photocatalysis and photoelectrochemistry still is the enlarging of its light-absorption area to the visible light wavelengths with the use of surface and volume doping by metal ions [1, 2]. Usually, such doping resulted in the decrease of functional activity of bare TiO₂, although the absorption area of doped TiO₂ increased noticeably.

Iron-doped TiO₂ nanoparticles were prepared using flame spray pyrolysis method, and performed rather high activity in photocatalytic mineralisation of oxalic acid under visible light illumination [3]. Features of Fe-TiO₂ photocatalysts (with variation of iron in the range of $0.005 < \text{Fe/Ti} < 0.3$) were investigated with CW X-band EPR, XRD and FTIR spectroscopy. Phase composition of the samples is shown in Fig. 1. Several different types of Fe(III) centers were distinguished: isolated paramagnetic centers exist in the samples with $0.005\% < \text{Fe/Ti} < 0.05$, which were attributed to high-spin Fe(III) ions ($S = 5/2$) in rhombic ligand fields state [4]. At $\text{Fe/Ti} \geq 10$, EPR spectra transformed to a broad single line, typical for Fe(III) ferromagnetic clusters (Fig.2).

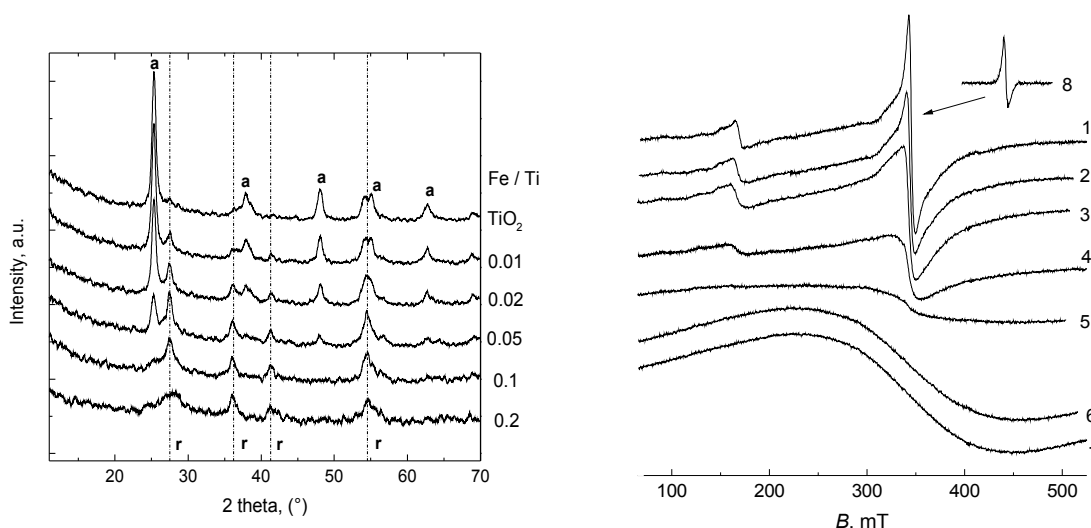


Fig. 1. XRD patterns of bare and Fe-doped TiO₂ at different Fe content. The anatase and rutile peaks are marked as (a) and (r, ---) respectively.

ESR spectra of Fe-doped TiO₂ photocatalysts at different Fe content: 1 – 0.5, 2 – 1.0, 3 – 2.0, 4 – 5.0, 5 – 10.0, 6 – 20.0, 7 – 30.0 at% Fe/TiO₂. 8 – obtained by subtraction of 2 from 1.

Kinetic curves of oxalic acid ($1 \cdot 10^{-4}$ M) decomposition at 25°C and $\lambda > 400$ nm on the bare and Fe-doped TiO_2 photocatalysts are given in Fig. 3. Interesting correlations (Fig. 4) were observed in comparison of EPR results with photocatalytic activity and the specific surface area $[S]$ data, which allowed us to assume that particularly the isolated Fe(III) centers are responsible for photomineralisation of oxalic acid, while the Fe(III) ferromagnetic aggregates (“clusters”) decrease the total efficiency of the system.

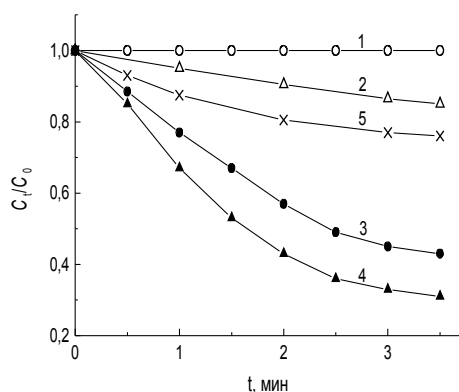


Fig. 3. Decomposition of oxalic acid ($1 \cdot 10^{-4}$ M) at 25°C and $\lambda > 400$ nm at different photocatalysts: 1 – bare TiO_2 , 2 – Degussa P25, Fe- TiO_2 with $[\text{Fe}]/[\text{Ti}] = 0.02$ (3), 0.05 (4), 0.2 (5). C_0 and C_t are carbon content in the solution at times 0 and t , correspondingly.

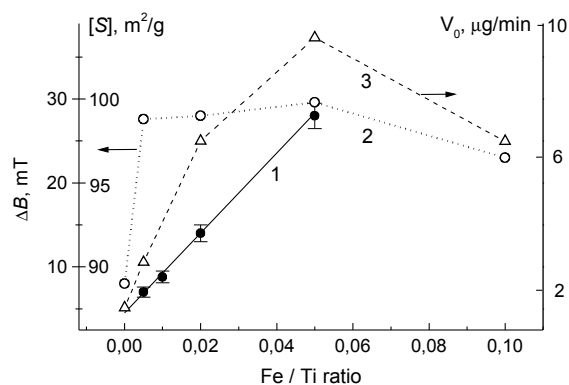


Fig. 4. The line width ΔB_{pp} (1) of paramagnetic Fe^{3+} centers in Fe-doped TiO_2 , specific surface area $[S]$ of the powders (2), and initial rates of photocatalytic mineralization of oxalic acid V_0 (3) vs. iron content.

In the paper, we'll report our experimental results on visible light photocatalysis on Fe-doped TiO_2 in comparison with the rest published data. The nature of defects and their dynamics under illumination will be also discussed.

Acknowledgement: This work was supported by RFBR Grant 08-03-00478.

References:

1. *Homogeneous and Heterogeneous Photocatalysis*, E. Pelizzetti and N. Serpone (Eds.), Reidel Publ. Co., Dordrecht (1986); Hoffmann M. R., Martin S. T., Choi W. and Bahnemann D.W. *Chem. Rev.*, **95**, 69-96 (1995).
2. Hoffmann M. R., Martin S. T., Choi W. and Bahnemann D.W. *Chem. Rev.*, **95**, No. 1, 69-96 (1995).
3. Teoch W. Y., Amal R., Maedler L., Pratsinis S. E. *Catal. Today*, **120**, 203-213 (2007).
4. Abragam A., Bleaney B. *Electron Paramagnetic Resonance of Transition Ions*. Oxford Univ. Press: London, New York, 1970.